Available online at www.sciencedirect.com

ScienceDirect

Procedia Manufacturing 30 (2019) 514–521

Procedia MANUFACTURING

www.elsevier.com/locate/procedia

14th Global Congress on Manufacturing and Management (GCMM-2018)

Parametric Study on Nanopattern Bactericidal Activity

Amar Velic[a]*, Tuquabo Tesfamichael[a], Zhiyong Li[a], Prasad K.D.V. Yarlagadda[a,b]

[a]*Science and Engineering Faculty, Queensland University of Technology, 2 George St, Brisbane 4000, Australia*
[b]*Institude of Health and Biomedical Innovation, Queensland University of Technology, 60 Musk Avenue, Kelvin Grove 4059, Australia*

Abstract

The ever-lurking threat of bacterial contamination and infection has seen a recent resurgence in line with the increasing ubiquity of biochemical resistance. Accordingly, intense research focus has been placed on the discovery of alternative mechanisms of action for antibacterial property. Nanopatterned surfaces, which operate on a physical mechanism of action, are showing great promise in this regard. That being said, the role of individual parameters in nanopattern bactericidal activity remains unclear. In this work, we develop a two-dimensional finite element model to study the interaction of a *Bacillus subtilis* cell with a nanopatterned surface in ABAQUS/Standard. Using our model, we analyze the effect of key physical parameters associated with pillar geometry and bacteria-surface interaction. Our results indicate that the localized deformational stresses generated within the bacterial peptidoglycan are sufficient to bring about catastrophic rupture and subsequent death. Moreover, we demonstrate that the most effective strategies for enhancing bactericidal efficiency are reducing pillar diameter and increasing attractive interaction. These findings can be used to guide the optimization of fabricated nanopatterned surfaces.

Keywords: nanopattern bactericidal activity; finite element method; geometry; bacteria-surface interaction

1. Introduction

Surface adhesion of bacteria triggers a biochemical cascade that metamorphoses an isolated cell into a complex, microcolony known as a 'biofilm' [1]. Biofilms confer enhanced resistance enabling its members to withstand physiological stresses that would otherwise overwhelm them in isolation. This makes biofilms notoriously difficult to

* Corresponding author. Tel.: +61 414 072 585.
E-mail address: a.velic@hdr.qut.edu.au

10.1016/j.promfg.2019.02.072

eradicate – a point best appreciated in the context of implant device infection which often necessitates costly and complicated revision surgery [2]. Accordingly, it is highly desirable to have surfaces resistant to bacterial adhesion.

The design of such surfaces is experiencing a drastic paradigm shift due to the increasing ubiquity of biochemical resistance. Traditional approaches for antibacterial property that use chemical functionalization underpinned by a biochemical mechanism of action are no longer effective [3]. Novel strategies are being pursued, and one of the most promising is nanopatterned surfaces. Originally inspired by insect wings, nanopatterned surfaces elicit bactericidal properties with a physical mechanism of action. More specifically, interaction between the bacteria and nanopattern causes deformation of the peptidoglycan, which leads to catastrophic rupture and subsequent leakage and death [4].

Despite intense research interest, a number of questions remain. Most pertinently, these pertain to the nature and role of the bacteria-surface interaction, and the effect of nanopattern geometry [5]. Accordingly, numerous attempts have been made to study these questions experimentally, though conclusions are weak or unclear. For instance, several experiments report that reduction to pillar diameter increases bactericidal efficiency, whilst drawing from data where pillar diameter, height and spacing are all simultaneously modified [6]. This is largely due to technological limitations which currently prevent accurate and repeatable control of individual geometrical parameters at the required resolution. Nevertheless, understanding the role and effect of interaction and geometry represents the key to unlocking the full potential of nanopatterned surfaces.

Accordingly, this works presents a technique to systematically study individual, key parameters involved in bacteria-nanopattern interaction, free of technological limitation and experimental intensiveness. To do so, we develop a two-dimensional finite element model in ABAQUS/Standard for the interaction of *Bacillus subtilis* cell with a nanopatterned surface. Using this model, we elucidate the effect of interaction force and pillar geometry (i.e. diameter, height and spacing) on deformational stress and bactericidal efficiency.

Nomenclature

D	diameter of nanopillars
S	spacing between nanopillars
H	height of nanopillars
F_0	interaction force at zero separation
E_P	elastic modulus of peptide crosslinks
E_G	elastic modulus of glycan strands
ν_{PG}	Poisson's ratio of glycan strands
UTS	ultimate tensile strength

2. Methodology

The deformation of a *B. subtilis* cell interacting with a nanopatterned surface was studied with a two-dimensional, finite element model using the ABAQUS/Standard implicit solver (Fig. 1). Developing the model required careful consideration of four aspects – materials, geometry, interaction and mesh generation. Some key parameters are summarized in Table 1.

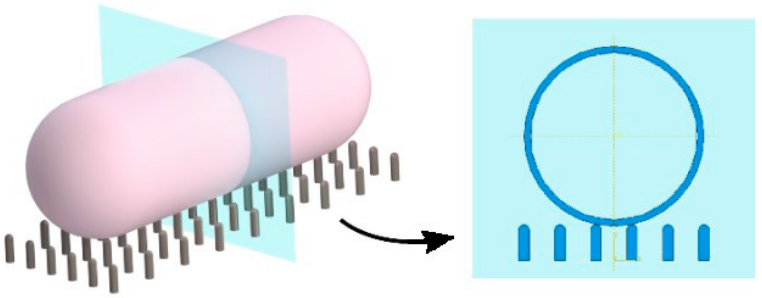

Fig. 1. Two-dimensional, plane strain simplification of bacteria-nanopattern interaction

Table 1. Key parameters for finite element model of bacteria-nanopattern interaction

Feature	Geometry	Material model	Mechanical properties	Element type	Global mesh size (nm)
Peptidoglycan	Thickness = 35nm [7] Outer diameter = 1μm [7]	Elastic	E = 115MPa ν = 0.118 [8, 9]	CP4ER (Plane strain)	1
Internal components	Outer diameter = 930 μm	N/A	N/A	R2D2 (Discrete rigid)	1
Nanopillars	Diameter (D): 20-80nm Spacing (S): 200-500nm Height (H): 200-500nm	N/A	N/A	R2D2 (Discrete rigid)	1

2.1. Materials

Physical rupture of peptidoglycan is the underlying cause of death in bacteria-nanopattern interaction [4]. Developing an appropriate material model for peptidoglycan material is thus critical for our simulation. Our model specifically pertains to the peptidoglycan of B. subtilis – a widely studied, gram-positive bacteria which is stiffer and more robust to the nanopattern mechanism than gram-negative counterparts [10]. Most accurately, peptidoglycan is a nonlinear material, owing to viscoelastic properties [11] and stress-stiffening behavior [12]. For 'small' deformations, however, peptidoglycan is approximately linear. Various AFM experiments have demonstrated linear force-indentation response to sinking depths of 250nm [13], and forces of 100pN [14]. Also, previous theoretical models of cell walls have used linear elastic approximations, showing good agreement with experimental results [8, 9, 13]. In this work, sinking depths are less than 250nm, and interaction forces are all in the order of 100pN, so a linear elastic approximation is appropriate. Peptidoglycan has mechanical properties that are directionally dependent, due to the disordered circumferential arrangement of glycan strands and peptide crosslinks [15]. For instance, glycan strands in the hoop direction have a higher stiffness than peptide crosslinks in the axial direction (i.e. $E_G > E_P$). For our simulation, the mechanical properties in the glycan direction are most relevant as they are in the plane of our two-dimensional model. To the best of our knowledge, however, E_G has not been previously reported for *B. subtilis*. Hence, we used available data for the elastic modulus in the peptide direction and an average of the ratio E_G / E_P from previous studies to infer the glycan properties. By this means, an elastic modulus of E_G = 115MPa was derived (Table 2). This is in the order of estimate by Tuson, et al. [16]. Based on the theoretical work of Assidi, et al. [8] and Gumbart, et al. [9] the average Poisson's ratio of peptidoglycan in the glycan direction is ν_{PG} = 0.118. Considering these factors, the peptidoglycan material was taken to be elastic and modelled with CPE4R (4-node, plane strain, quadrilateral, reduced integration) elements with mechanical properties listed in Table 2.

Table 2. Elastic moduli of peptidoglycan

Reference	Bacteria	Gram-stain	E_P (MPa)	E_G (MPa)	$E_G : E_P$
[17]	*E. coli*	Negative	30	35	1.17
			15	60	4
[8]	N/A		3	32	10.67
			5	10	2
[12]	*E. coli*	Negative	23	49	2.13
[9]	*E. coli*	Negative	4	11.4	2.85
			17.5	66.3	3.79
[18]	*B. subtilis*	Positive	30	(~115)	

The various materials of components internal to the cell wall (i.e. plasma membrane, cytoplasm and intracellular structures) were neglected and internal features were simplified as a discrete rigid wire constrained with a surface-to-surface tie at the internal diameter of the peptidoglycan. This restricted the global shape change of the bacteria during interaction and confined the deformation to the peptidoglycan layer, mimicking the effect of high-turgor pressure in gram-positive bacteria [11].

Lastly, the material of the pillars was also considered to be rigid. This simplification was permitted due to the order of magnitude difference between the stiffness of gram-positive peptidoglycan (~100MPa) and materials commonly used for nanopatterns fabrication such as titanium (~100Gpa) [19] and black silicon (~100Gpa) [20]. Deformation of the pillars is thus considered negligible relative to the deformation of the peptidoglycan, having minimal influence on our results.

2.2. Geometry

Like its mechanical properties, the dimensions of peptidoglycan depend on turgor state, hydration state and immobilization method. For the case of intact, turgored and hydrated B. subtilis cells, an outer diameter of 1µm and thickness of 35nm are observed using cryogenic electron microscopy techniques [7]. These values were used in our model as the experimental conditions mimic those *in vivo*.

Nanopillars were modelled as round-capped cylinders, spaced equally to form an organised nanopattern. The nanopattern can thus be defined entirely by three geometric parameters – pillar diameter (D), height (H) and spacing (S). Our original simulations were carried out with dimensions of D = 60nm, H = 200nm and S = 200nm to imitate the wing nanopattern of *Psaltoda claripennis* which is an established natural model for biomimetic design [21]. Diameter was subsequently varied between 20-80nm, with the lower bound reflecting the resolution that can be achieved with some fabrication techniques, though not with great uniformity or control [22]. Pillar spacing was varied from 200nm to an upper limit of 500nm, as further spacing approached the scenario where the cell contacted the substrate before the pillars (i.e. no suspension). Pillar height was also varied between 200-500nm (Table 1).

2.3. Interaction

Bacteria-surface interaction can be described in two phases. The first phase pertains to initial approach and immediate contact, during which physicochemical properties generate distance-dependent attractive or repulsive interactions in the order of 100pN [23-25]. The second phase pertains to adsorption after contact, during which molecular and cellular interactions generate time-dependent adhesive forces, typically in the order of 1nN [26]. Given that these adhesive forces are 'reactive', the 'action' forces in the first phase are of greater interest for our model. The precise value and nature of the interaction forces during this phase is a complex interplay of physicochemical properties, such as the surface hydrophobicity and charge of the bacteria and substrate, and the pH and ionic strength of the surrounding aqueous medium. Approach forces for *B. subtilis* interacting with a nanopatterned surface have not been reported, though various observations support an approach that is attractive in nature. For instance, nanopatterned surfaces are superhydrophobic, owed to their physical topography [20]. High levels of hydrophobicity are strongly correlated to physicochemical attraction, due to ease with which interfacial water is eliminated [24]. Also, various studies have shown increased numbers of adhered bacteria on nanopatterned surfaces versus flat controls [27]. Lastly, Harimawan, et al. [26] demonstrated adhesive retraction forces of 1.488nN for *B. subtilis* on stainless steel 316. Favorable attractive forces in the first phase of interaction are typically a precursor to adhesive forces developed in the second phase. Accordingly, for *B. subtilis*-nanopattern interaction we take a conservative estimate of 100pN per contacted pillar (i.e. 200pN) of attractive force at zero separation (i.e. F_0).

In ABAQUS/Standard, this interaction was modelled as a surface-to-surface contact with 'hard' normal behaviour and relatively low isotropic, tangential friction coefficient (0.1) [28]. This was carried out in two steps. In the first step, the bacteria cell was brought into contact with the nanopattern with a very small sinking depth (i.e. 0.05nm). Stresses generated in this step were more than a magnitude smaller than those in the second step. The small, initial contact was necessary to achieve convergence in the second step, in which a downward concentrated force was applied at the reference point of the rigid centre to simulate the interaction force (F_0). Exactly similar results were also obtained using a body force load type.

2.4. Mesh generation

Peptidoglycan was meshed with CPE4R elements generated by a medial axis algorithm with minimized mesh transitions. Other, rigids parts were meshed with R2D2 (2-node, plane strain, linear link) elements. The density of the mesh was controlled by adjusting approximate size with the global seed controls. By this means, a convergence study

was also carried out. This study indicated that a mesh-independent solution could be achieved confidently using elements of approximately 1nm, which produced about 180,000 elements and a reasonable CPU time of around 3.5 minutes (Fig. 2).

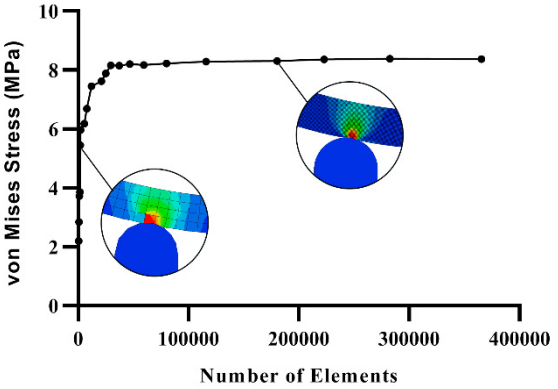

Fig. 2. Mesh convergence study

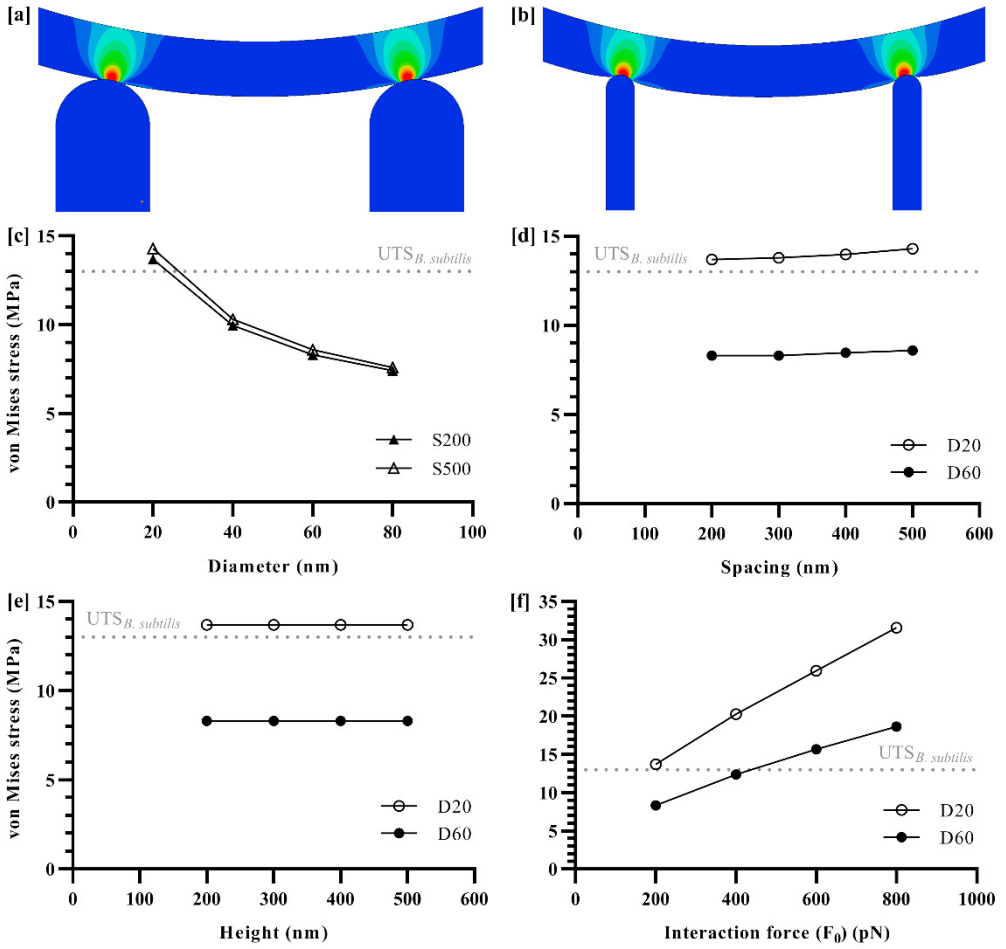

Fig. 3. Parametric study of deformational stress on peptidoglycan in *B. subtilis*-nanopattern interaction. Visualisation of deformation and stress contour for interaction with pillars of diameter (a) 60nm and (b) 20nm (S = 200nm, H = 200nm, F_0 = 200pN). (c) Effect of pillar diameter on maximum von Mises stress at spacing of 200nm and 500nm (H = 200nm, F_0 = 200pN) (d) Effect of pillar spacing on maximum von Mises stress with pillars of diameter 60nm and 20nm (H = 200nm, F_0 = 200pN) (e) Effect of pillar height on maximum von Mises stress with pillars of diameter 60nm and 20nm (S = 200nm, F_0 = 200pN) (f) Effect of interaction force on maximum von Mises stress with pillars of diameter 60nm and 20nm (H = 200nm, S = 200nm)

3. Results and discussion

Our model was used to conduct a parametric study, with results displayed in Fig. 3. As the bacteria interacts with the nanopattern, its peptidoglycan layer deforms to the contours of the pillars in the contact region (Fig. 3a). This is easily visible for narrower pillars, in which case the shape change is more pronounced (Fig. 3b). Our results suggest that the stresses accompanying this local deformation are of several megapascals. These stresses are interpreted in the context of a prevailing theory on nanopattern biocide that postulates that local deformation stresses kill the bacteria by piercing its peptidoglycan [22, 29, 30]. More accurately, the stress exceeds the ultimate tensile strength (UTS) of the peptidoglycan initiating local failure that propagates until catastrophic rupture. Studying hydrated cellular 'thread', Thwaites and Surana [18] found an ultimate tensile strength of 13MPa for *B. subtilis*. This is in the same order of stresses predicted by our model, reinforcing that physical – not biochemical - mechanisms underpin the bactericidal effect. Our results further indicate that this bactericidal effect can be enhanced or suppressed by controlling key physical parameters of the interaction.

3.1. Effect of pillar diameter

When a diameter of 60nm is used in our model – imitating the pillar geometry found on the wings of *P. claripennis* – a maximum stress of approximately 8MPa is generated within the peptidoglycan. This would suggest that the nanopattern geometry is ineffective against *B. subtilis*, which has a tensile strength of 13MPa. Indeed, this mimics a common experimental finding that gram-positive bacteria are mechanically robust to insect wing nanopatterns due to reinforced peptidoglycan [3]. Our model predicts that reducing pillar diameter to at least 20nm is required to affect *B. subtilis* bacteria (Fig. 3c). This is part of a trend whereby reducing nanopillar diameter causes an exponential increase in the stress developed within the peptidoglycan layer. This should be accompanied by enhanced killing efficiency – a trend which indeed demonstrated in numerous experimental studies [6, 22, 30, 31]. Some theoretical models also agree [32]. Our observations are most likely due to the reduction in interfacial contact with narrower pillars, which distributes the interaction forces over a smaller area and intensifies stress. Evidently, reducing pillar diameter seems to be a very viable strategy for enhancing the effectiveness of manufactured nanopatterned surfaces.

3.2. Effect of pillar spacing

Increased pillar spacing results in minor enhancement to maximum stress within the peptidoglycan layer (Fig. 3d). This is, however, most likely an 'artifact' from the contact geometry that has a greater tangential component in the case of large spacings. Conversely, experimental findings mostly suggest that decreasing spacing elicits increased killing efficiency [6, 30]. This is attributed to an increase in the number of contact points with closely packed pillars [31]. In these experiments, however, the effect of spacing is not properly isolated, hence the conclusions are not robust. In our two-dimensional interaction model, the cell only ever contacts two pillars, even when very small spacing is applied. Expanding the model to 3D in to account for the numerous pillars along the length of the bacteria may provide better insight into the role of pillar spacing.

3.3. Effect of pillar height

Our data indicates that deformational stress is independent of pillar height (Fig. 3e), so long as there is total suspension of the bacteria (i.e. pillars at least ~50nm tall). This would imply that the killing efficiency of a nanopattern is insensitive to changes in pillar height. This result is at odds with an overwhelmingly popular experimental observation that taller pillars enhance bactericidal property [6, 22, 31, 33]. Though these studies do not effectively decouple the contributions of individual geometric parameters, pillar height certainly seems to play some role. A possible theory is that pillar height modulates interaction forces between the bacteria and the underlying substrate, eliminating some short distance repulsion and increasing attractive interaction force [27]. The modulation of interaction force by height is not captured by our model, though we do demonstrate that interaction force strongly affects deformational stress, as discussed further below. Thus, a more comprehensive, distance-dependent description of the interaction forces using DLVO theory may provide more accurate and verifiable results.

3.4. Effect of interaction force

Interaction force has a direct, linear effect on the stress developed within the peptidoglycan (Fig. 3f). For example, a nanopattern comprising 60nm diameter pillars that is normally innocuous to gram-positive bacteria has lethal effects when interaction force is increased beyond approximately 400pN. An analogous linear trend is also reported by Li [34], using a theoretical model of nanopattern adhesion based on a surface thermodynamics approach. This effect is also demonstrated experimentally by Nowlin, et al. [27] studying two strains of *Saccharomyces cerevisiae*. In this study, the stronger adhering strain was killed with increased efficiency. Taken together, these results imply that nanopattern killing efficiency can be improved by enhancing attractive interaction via control of physicochemical surface properties to increase hydrophobicity [25] and/or decrease surface charge [24] for example. This could be a viable strategy for manufacturing.

In addition, our results suggest that interaction force in the order of 100pN is the minimum required to generate stresses sufficient to rupture the peptidoglycan layer. For example, applying the effective weight of the bacteria in simulated body fluid ($\rho_{B.subtilis}$ = 1.22 g/cm^3, ρ_{SBF} = 1.02 g/cm^3) to our model generated deformational stresses of only several kilopascals. This seems highly unlikely to cause rupture, implying that the interaction between bacteria and nanopattern is not merely gravitational. This brings into question the validity of earlier conceptual models which postulated that the bacteria would deform under its own weight.

Due to the scale and resolution of this interaction, the value of our results simply cannot be verified with certainty. Their accuracy is also limited by a number of assumptions. For instance, the exact values for cell diameter, peptidoglycan thickness, mechanical property and interaction force can vary substantially and are highly dependent on growth phase [35], hydration state [18], turgor state [12], surrounding medium [24] and immobilization method [36]. Whilst care was taken to use values that would mimic the physiological state *in vivo*, some discrepancy is to be expected. In addition, our model neglects extracellular structures, such as pili and flagella, which can act as surface sensors that behave actively [37]. This is inherent to the difficulty of simulating a highly dynamic and active biological problem as a static, mechanical one. That being said, the predicted trends seem highly valid in the context of previous experimental findings. Thus, our results provide strategies to improve the manufacture of enhanced nanopatterned surface for antibacterial application.

4. Conclusion

In this work, ABAQUS/Standard was applied to study a two-dimensional finite element model for the interaction of a *B. subtilis* cell with a nanopatterned surface. We demonstrate that the localized deformation stresses generated in the peptidoglycan are sufficient to cause rupture and subsequent death. This model also provided an efficient method to study the isolated effects of key interaction parameters such as pillar geometry and interaction force. Our results suggest that the most effective strategies for increasing the bactericidal efficiency of nanopatterned surfaces are to reduce pillar diameter and enhance attractive interaction. Pillar height and spacing were not significant parameters in our model, though future improvements are proposed to better account for their possible effects. Our work serves as a guide to optimize the manufacture of nanopatterned surfaces.

Acknowledgements

The author would like to acknowledge the Queensland University of Technology for funding this research via the Research Training Program (RTP) stipend.

References

[1] W. M. Dunne, "Bacterial Adhesion: Seen Any Good Biofilms Lately?," *Clinical Microbiology Reviews,* vol. 15, no. 2, pp. 155-166, 2002.
[2] M. Ribeiro, F. J. Monteiro, and M. P. Ferraz, "Infection of orthopedic implants with emphasis on bacterial adhesion process and techniques used in studying bacterial-material interactions," *Biomatter,* vol. 2, no. 4, pp. 176-194, 2012.
[3] J. Hasan, R. J. Crawford, and E. P. Ivanova, "Antibacterial surfaces: the quest for a new generation of biomaterials," *Trends in Biotechnology,* vol. 31, no. 5, pp. 295-304, 5// 2013.
[4] S. Pogodin *et al.*, "Biophysical Model of Bacterial Cell Interactions with Nanopatterned Cicada Wing Surfaces," *Biophysical Journal,* vol. 104, no. 4, pp. 835-840, 19/02/2013 2013.
[5] A. Elbourne, R. J. Crawford, and E. P. Ivanova, "Nano-structured antimicrobial surfaces: From nature to synthetic analogues," *Journal of*

Colloid and Interface Science, vol. 508, pp. 603-616, 2017/12/15/ 2017.
[6] C. M. Bhadra *et al.*, "Subtle Variations in Surface Properties of Black Silicon Surfaces Influence the Degree of Bactericidal Efficiency," *Nano-Micro Letters,* vol. 10, no. 2, p. 36, 2018/02/06 2018.
[7] V. R. F. Matias and T. J. Beveridge, "Cryo-electron microscopy reveals native polymeric cell wall structure in Bacillus subtilis 168 and the existence of a periplasmic space," *Molecular Microbiology,* vol. 56, no. 1, pp. 240-251, 2005/04/01 2005.
[8] M. Assidi, F. Dos Reis, and J. F. Ganghoffer, "Equivalent mechanical properties of biological membranes from lattice homogenization," *Journal of the Mechanical Behavior of Biomedical Materials,* vol. 4, no. 8, pp. 1833-1845, 2011/11/01/ 2011.
[9] J. C. Gumbart, M. Beeby, G. J. Jensen, and B. Roux, "Escherichia coli Peptidoglycan Structure and Mechanics as Predicted by Atomic-Scale Simulations," *PLOS Computational Biology,* vol. 10, no. 2, p. e1003475, 2014.
[10] J. Hasan *et al.*, "Selective bactericidal activity of nanopatterned superhydrophobic cicada Psaltoda claripennis wing surfaces," *Applied Microbiology and Biotechnology,* vol. 97, no. 20, pp. 9257-9262, 2013// 2013.
[11] V. Vadillo-Rodríguez and J. R. Dutcher, "Viscoelasticity of the bacterial cell envelope," *Soft Matter,* 10.1039/C0SM01054E vol. 7, no. 9, pp. 4101-4110, 2011.
[12] Y. Deng, M. Sun, and J. W. Shaevitz, "Direct Measurement of Cell Wall Stress Stiffening and Turgor Pressure in Live Bacterial Cells," *Physical Review Letters,* vol. 107, no. 15, p. 158101, 10/06/ 2011.
[13] M. Arnoldi, M. Fritz, E. Bäuerlein, M. Radmacher, E. Sackmann, and A. Boulbitch, "Bacterial turgor pressure can be measured by atomic force microscopy," *Physical Review E,* vol. 62, no. 1, pp. 1034-1044, 07/01/ 2000.
[14] X. Yao *et al.*, "Atomic force microscopy and theoretical considerations of surface properties and turgor pressures of bacteria," *Colloids and Surfaces B: Biointerfaces,* vol. 23, no. 2, pp. 213-230, 2002/02/01/ 2002.
[15] L. Gan, S. Chen, and G. J. Jensen, "Molecular organization of Gram-negative peptidoglycan," *Proceedings of the National Academy of Sciences of the United States of America,* vol. 105, no. 48, pp. 18953-18957, 2008.
[16] H. H. Tuson *et al.*, "Measuring the stiffness of bacterial cells from growth rates in hydrogels of tunable elasticity," *Molecular Microbiology,* vol. 84, no. 5, pp. 874-891, 05/02 2012.
[17] X. Yao, M. Jericho, D. Pink, and T. Beveridge, "Thickness and elasticity of gram-negative murein sacculi measured by atomic force microscopy," *Journal of bacteriology,* vol. 181, no. 22, pp. 6865-6875, 1999.
[18] J. J. Thwaites and U. C. Surana, "Mechanical properties of Bacillus subtilis cell walls: effects of removing residual culture medium," *Journal of bacteriology,* vol. 173, no. 1, pp. 197-203, 1991.
[19] J. Hasan, S. Jain, and K. Chatterjee, "Nanoscale Topography on Black Titanium Imparts Multi-biofunctional Properties for Orthopedic Applications," *Scientific Reports,* Article vol. 7, p. 41118, 01/23/online 2017.
[20] J. Hasan, S. Raj, L. Yadav, and K. Chatterjee, "Engineering a nanostructured "super surface" with superhydrophobic and superkilling properties," *RSC Advances,* 10.1039/C5RA05206H vol. 5, no. 56, pp. 44953-44959, 2015.
[21] E. P. Ivanova *et al.*, "Natural Bactericidal Surfaces: Mechanical Rupture of Pseudomonas aeruginosa Cells by Cicada Wings," *Small,* vol. 8, no. 16, pp. 2489-2494, 2012.
[22] M. Michalska *et al.*, "Tuning antimicrobial properties of biomimetic nanopatterned surfaces," *Nanoscale,* 10.1039/C8NR00439K vol. 10, no. 14, pp. 6639-6650, 2018.
[23] Q. Huang, H. Wu, P. Cai, J. B. Fein, and W. Chen, "Atomic force microscopy measurements of bacterial adhesion and biofilm formation onto clay-sized particles," *Scientific Reports,* Article vol. 5, p. 16857, 11/20/online 2015.
[24] Y.-L. Ong, A. Razatos, G. Georgiou, and M. M. Sharma, "Adhesion Forces between E. coli Bacteria and Biomaterial Surfaces," *Langmuir,* vol. 15, no. 8, pp. 2719-2725, 1999/04/01 1999.
[25] J. M. Thwala, M. Li, M. C. Y. Wong, S. Kang, E. M. V. Hoek, and B. B. Mamba, "Bacteria–Polymeric Membrane Interactions: Atomic Force Microscopy and XDLVO Predictions," *Langmuir,* vol. 29, no. 45, pp. 13773-13782, 2013/11/12 2013.
[26] A. Harimawan, A. Rajasekar, and Y.-P. Ting, "Bacteria attachment to surfaces – AFM force spectroscopy and physicochemical analyses," *Journal of Colloid and Interface Science,* vol. 364, no. 1, pp. 213-218, 2011/12/01/ 2011.
[27] K. Nowlin, A. Boseman, A. Covell, and D. LaJeunesse, "Adhesion-dependent rupturing of Saccharomyces cerevisiae on biological antimicrobial nanostructured surfaces," *Journal of the Royal Society Interface,* vol. 12, no. 102, p. 20140999, recieved (09/05/15), accepted (11/03/15) 2015.
[28] J. L. Lopes *et al.*, "Friction and wear behaviour of bacterial cellulose against articular cartilage," *Wear,* vol. 271, no. 9, pp. 2328-2333, 2011/07/29/ 2011.
[29] P. L. Denver, N. Huu Khuong Duy, M. B. Chris, J. Saulius, and P. I. Elena, "Influence of nanoscale topology on bactericidal efficiency of black silicon surfaces," *Nanotechnology,* vol. 28, no. 24, p. 245301, 2017.
[30] M. N. Dickson, E. I. Liang, L. A. Rodriguez, N. Vollereaux, and A. F. Yee, "Nanopatterned polymer surfaces with bactericidal properties," *Biointerphases,* vol. 10, no. 2, p. 021010, 06/15 2015.
[31] S. M. Kelleher *et al.*, "Cicada Wing Surface Topography: An Investigation into the Bactericidal Properties of Nanostructural Features," *ACS Applied Materials and Interfaces,* vol. 8, no. 24, pp. 14966-14974, 2016.
[32] F. Xue, J. Liu, L. Guo, L. Zhang, and Q. Li, "Theoretical study on the bactericidal nature of nanopatterned surfaces," *Journal of Theoretical Biology,* vol. 385, pp. 1-7, 11/21/ 2015.
[33] D. P. Linklater *et al.*, "High Aspect Ratio Nanostructures Kill Bacteria via Storage and Release of Mechanical Energy," *ACS Nano,* 2018/05/31 2018.
[34] X. Li, "Bactericidal mechanism of nanopatterned surfaces," *Physical Chemistry Chemical Physics,* 10.1039/C5CP05646B vol. 18, no. 2, pp. 1311-1316, 2016.
[35] M. G. Sargent, "Control of cell length in Bacillus subtilis," *Journal of bacteriology,* vol. 123, no. 1, pp. 7-19, 1975.
[36] V. Vadillo-Rodríguez *et al.*, "Comparison of Atomic Force Microscopy Interaction Forces between Bacteria and Silicon Nitride Substrata for Three Commonly Used Immobilization Methods," *Applied and Environmental Microbiology,* vol. 70, no. 9, p. 5441, 2004.
[37] G. A. O'Toole and G. C. L. Wong, "Sensational biofilms: surface sensing in bacteria," *Current opinion in microbiology,* vol. 30, pp. 139-146, 03/08 2016.